Supplementary Data

Visualization of penicillin G acylase in bacteria and high-throughput screening of inhibitors using a ratiometric fluorescent probe

Lu Li,[a,b,‡] Lei Feng,[b,c,‡] Ming Zhang,[b,‡] Xin He,[b] Shengqiao Luan,[b] Chao Wang,*[,b] Tony D. James,*[,d] Houli Zhang,[b] Huilian Huang,[e] and Xiaochi Ma*[,a]

[a] Jiangsu Key Laboratory of New Drug Research and Clinical Pharmacy, Xuzhou Medical University, Xuzhou 221004, China

E-mail: maxiaochi2019@163.com (X.C. Ma)

[b] College of Pharmacy, Academy of Integrative Medicine, The National & Local Joint Engineering Research Center for Drug Development of Neurodegenerative Disease, Dalian Medical University, Dalian 116044, China

E-mail: wach_edu@sina.com (C. Wang)

[c] State Key Laboratory of Fine Chemicals, Dalian University of Technology, Dalian 116024, China

[d] Department of Chemistry, University of Bath, Bath BA2 7AY, UK.

E-mail: t.d.james@bath.ac.uk (T.D. James)

[e] Laboratory of Modern Preparation of TCM, Ministry of Education, Jiangxi University of Traditional Chinese Medicine, Nanchang 330004, China

Content

Experimental section

Materials and instruments. All the chemical reagents such as chloroform, acetonitrile, and methanol were purchased from Tianjin Kemio Chemical Reagent Co., Ltd. Recombinant human Carboxylesterases (CES1b, CES1c, and CES2) were purchased from Corning Incorporated Life Sciences. Lipase, dipeptidyl peptidase 8, Bovine serum albumin, Human albumin, proline aminopeptidase, and penicillin G acylase were purchased from sigma-aldrich.

NMR spectra were measured using Bruker-600, 500 with tetramethylsilane (TMS) as the internal standard (Bruker, USA). High resolution mass spectral (HRMS) analyses were measured with G6224A TOF-MS. Constant temperature incubator shaker (HZQ-C) was the production of Harbin Donglian Electronic Technology Development Co., LTD. Fluorescence confocal microscopic imaging was conducted with Leica (German). The bioassay solutions in 96-well plates were analyzed using a BioTek Synergy H1 microplate reader (BioTek, USA). The fluorescence imaging of 96-well plate was recorded using Amersham Typhoon RGB (GE, USA).

Synthesis of *N*-(n-butyl)-4-*N*-phenylacetamide-1, 8-naphthalimide (PNA)

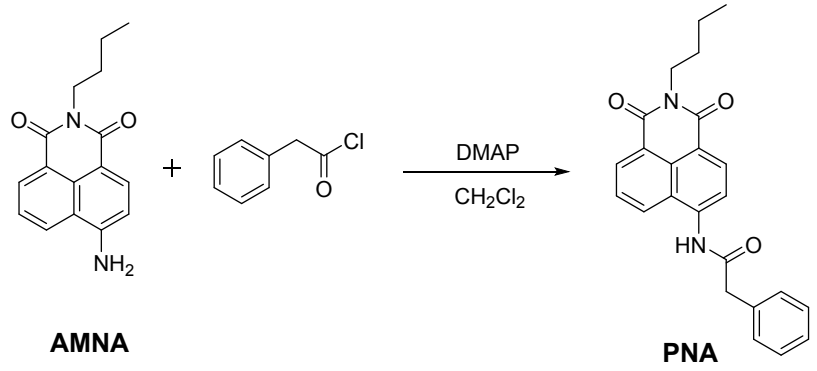

AMNA **PNA**

Scheme S1. Synthetic route for the fluorescent probe **PNA**.

To a solution of 67 mg 4-amino-*N*-n-butyl-1,8-naphthalimide (**AMNA**, 0.25 mmol) and 37 mg 4-dimethylaminopyridine (**DMAP**) (0.30 mmol) in 30 mL of CH_2Cl_2, phenylacetyl chloride (0.5 mmol, mixed with 5 mL of CH_2Cl_2) was added dropwise at 0 °C in 30 min. After being stirred at this temperature for 1 h, the mixture was warmed to room temperature and stirred overnight. The solvent was removed *in vacuo*, and the residual solid was purified by chromatography (silica gel, dichloromethane as eluent) to afford 42 mg (43%) of **PNA** as a light yellow solid. The structure of **PNA** was confirmed by ^{1}H NMR, ^{13}C NMR, and HRMS (Figures S13−15), and the data are as follows: ^{1}H NMR (600 MHz, DMSO-d_6) δ 10.61 (s, 1H), 8.69 (dd, J = 8.5, 0.7 Hz, 1H), 8.53 (dd, J = 7.2, 0.7 Hz, 1H), 8.46 (d, J = 8.2 Hz, 1H), 8.27 (d, J = 8.2 Hz, 1H), 7.90 (dd, J = 8.4, 7.4 Hz, 1H), 7.44 (d, J = 7.2 Hz, 2H), 7.38 (dd, J = 10.5, 4.8 Hz, 2H), 7.29 (t, J = 7.4 Hz, 1H), 4.09 – 4.00 (m, 2H), 3.95 (s, 2H), 1.69 – 1.56 (m, 2H), 1.42 – 1.32 (m, 2H), 0.93 (t, J = 7.4 Hz, 3H). ^{13}C NMR (150 MHz, DMSO-d_6) δ 170.85, 163.94, 163.38, 140.56, 136.14, 132.02, 131.37, 129.76, 129.62, 128.88, 128.79, 127.16, 127.00, 124.72, 122.83, 120.28, 118.26, 43.44, 30.14, 20.28, 14.21. HR-MS: *m/z* 499.1488 $[M+CF_3COO]^-$ (cal. 499.1481 $C_{26}H_{22}F_3N_2O_5$).

The hydrolysis of PNA mediated by bacterial PGA

The ratiometric fluorescent probe **PNA** was hydrolyzed by PGA, which yielded **AMNA**. The bacterial PGA (0.05 U/mL) was dissolved in 200 μL phosphate buffer (pH 7.4) together with **PNA** (10 μM), which was co-incubated at 37 ºC for 30 min. **PNA** (10 μM) was prepared when the **PNA** stock solution (2 mM, DMSO) was added

into the phosphate buffer with the DMSO volume < 1%, which could improve the solubility of **PNA** and keep the activity of PGA. Then, 100 μL acetonitrile was added into the incubated solution to terminate the enzymatic reaction. The fluorescence spectra of the reaction solutions as well as fluorescence intensity using BioTek Synergy H1 microplate reader (λ_{ex} 400/λ_{em} 470 nm and λ_{ex} 400/λ_{em} 540 nm). The enzymatic reaction solution was analyzed for the production of **AMNA** using HPLC (40% – 100% methanol, 0 – 30 min, flow rate 0.8 mL/min).

Fluorescence responses of **PNA** (10 μM) to different concentrations of PGA were performed upon addition of increasing concentration of PGA (0 – 0.2 U/mL) in phosphate buffer (pH 7.4) for 30 min. While, fluorescence responses of **PNA** (10 μM) towards incubation time were evaluated upon the addition of PGA (0.05 U/mL) in phosphate buffer for incubation time 0 – 80 min with acetonitrile (33%, *v/v*) to terminate the enzymatic reaction (λ_{ex} 400/λ_{em} 470 nm, λ_{ex} 400/λ_{em} 540 nm, 37 ˚C). The linear relationship was analyzed on the basis of the fluorescence intensities ratio (I_{540}/I_{470}) corresponding to the amount of **PNA** and **AMNA**, respectively.

Selectivity of the hydrolysis of PNA mediated by PGA.

The enzymatic selective experiments towards different enzymes (100 μg/mL) were preformed according to the enzymatic reaction conditions, including human Carboxylesterase (CES1b, CES1c, and CES2), DPP8, PAP peptidase, and proteins BSA, HSA. The fluorescence intensity for each group was measured and the fluorescence intensity ratio values were obtained for the selective evaluation in comparison with that of the co incubation between **PNA** and PGA.

Interference of various species on the fluorescence intensity of PNA and the hydrolysis of PNA mediated by PGA.

The fluorescence intensity ratio (I_{540}/I_{470}) was studied on the basis of the fluorescence intensity (λ_{ex} 400/λ_{em} 470 nm, λ_{ex} 400/λ_{em} 540 nm). The influence of ions on the fluorescence emission of **PNA** and **AMNA** and the hydrolysis activity of PGA were measured in the presence of K^+, Fe^{3+}, Ba^{2+}, Ca^{2+}, Na^+, Mn^{2+}, Zn^{2+}, Ni^{2+}, Cr^{3+}, Cu^{2+}, NO_3^-, Ca^{2+}, CO_3^{2-}, Sn^{2+}, SO_4^{2-} (each 200 μM). Similarly, the influence of amino acids on the fluorescence intensities of **PNA** and **AMNA** and the hydrolysis

capability of bacterial PGA were evaluated in the presence of various amino acids, such as Leu, Ala, Pro, Phe, Met, Asp, Lle, Thr, His, Val, Asn, Glu (10 μM).

Kinetic behavior of the hydrolysis of PNA mediated by PGA.

In order to estimate the kinetic parameters of **PNA** mediated by PGA, the reaction kinetics were performed. Briefly, **PNA** (0 − 60 μM) was incubated with PGA for 30 min which ensured less than 20% of substrate was metabolized, and the formation rates of **AMNA** were in relation to incubation time and protein concentration in the linear range. The **PNA** stock solution was prepared to be 2 mM in DMSO, which was added into the PGA enzymatic reaction system with DMSO < 1%. The apparent K_m and V_{max} values were calculated from nonlinear regression analysis of experimental data according to the followed equation.

$$v = \frac{V_{max} \times [S]n}{K_m + [S]n} \quad \text{.....(1)}$$

The V_{max} represents the maximum rate and K_m is the substrate concentration at the half-maximal rate.

Fluorescence imaging of bacteria on the basis of the endogenous PGA.

In the present work, **PNA** was incubated with four Gram-positive bacteria strains, including *Staphylococcus aureus* DSM 3463, *Lactobacillus acidophilus*, *Lactobacillus amylophilus*, and *Lactobacillus salivarius* for 2 hours to get the fluorescence images by confocal laser scanning microscopy. These bacteria were culutred in Luria-Bertani (LB) medium for 24 h to get enough bacteria cells with OD value 0.8. Then, **PNA** (50 μM) was added into the culture for a co-incubation with bacteria for 2 h at 37 ºC. After the clean out of the medium by centrifugation, the bacterial cells were suspended in phosphate buffer (pH 7.4) solution, which were dropped on glas slides for imaging experiment. The bacteria were imaged using a Confocal Microscope with λ_{ex} 405/λ_{em} 425 − 459 nm for **PNA**, λ_{em} 525 − 575 nm for **AMNA**. To study the enzyme specificity, the bacteria were pretreated with enzyme

inhibitor oleanolic acid (50 μM) along with the co-incubation of **PNA** (50 μM) for imaging studies.

Inhibitor screening of PGA using the established high-throughput screening system.

36 natural compounds from a natural compounds library belonging to various natural compound skeletons according to natural compound chemistry have been screened for their inhibitory effect on bacterial PGA. When PGA (0.1 U/mL) and **PNA** (10 μM) were co-incubated in 96-well plate, 36 natural compounds were added into the incubation solution at the concentration 100 μM. After the co-incubation of 30 min, the plate was imaged by Amersham Typhoon RGB for the sensing of **AMNA** (λ_{ex} 473 nm/λ_{em} 550 − 590 nm). Additionally, the fluorescence intensity of each well in the plate was measured by BioTek Synergy H1 microplate reader. Finally, the IC_{50} value of oleanolic acid as a potential PGA inhibitor was determined on the basis of the inhibitory effect at different concentrations.

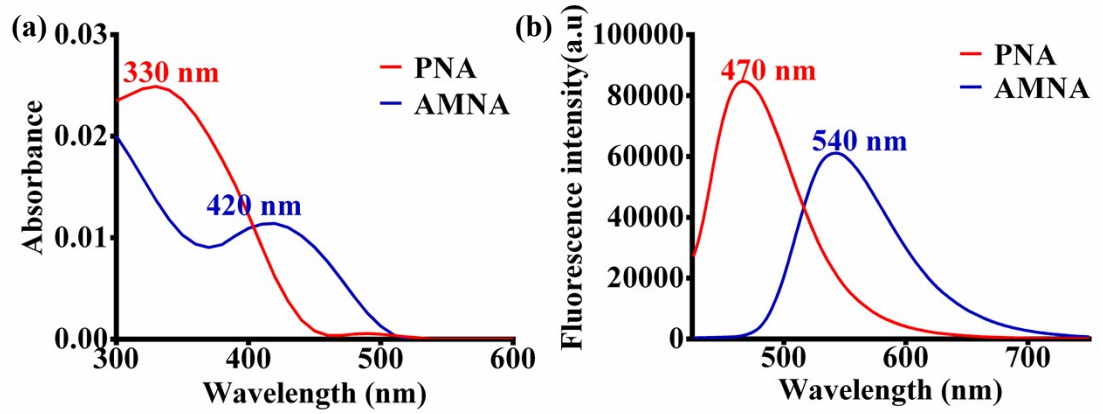

Fig. S1. The absorption spectra (a) and fluorescence spectra (b) of **PNA** and **AMNA**.

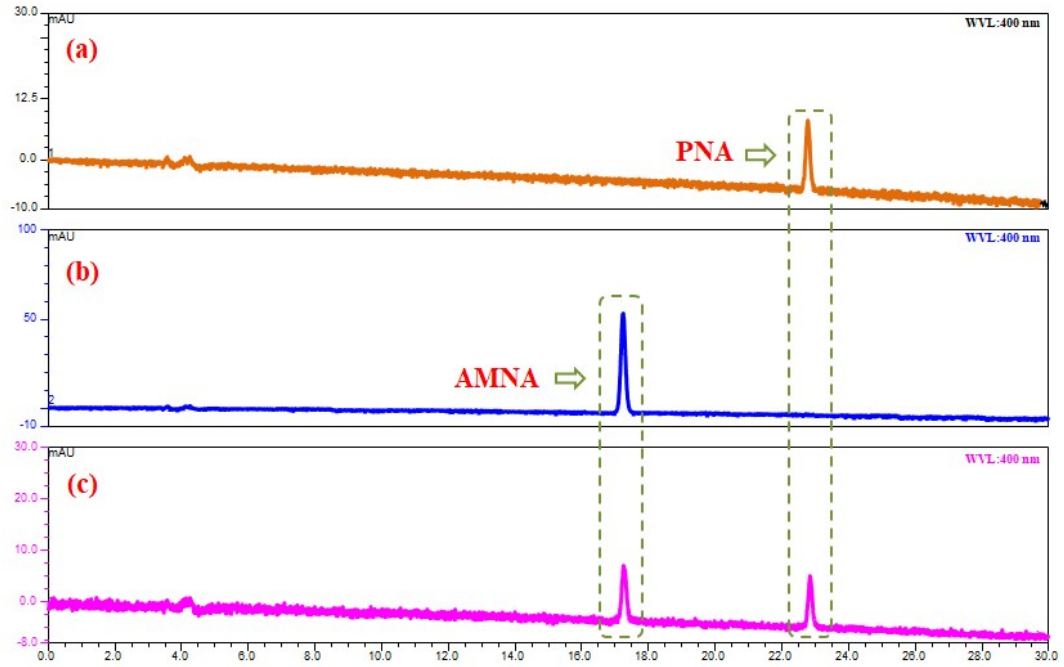

Fig. S2. The HPLC-DAD chromatograms for the enzymatic reaction of the fluorescent probe **PNA** mediated by PGA. (a) The standard reference **PNA**. (b) The standard reference **AMNA**. (c) The co-incubation solution of **PNA** and PGA.

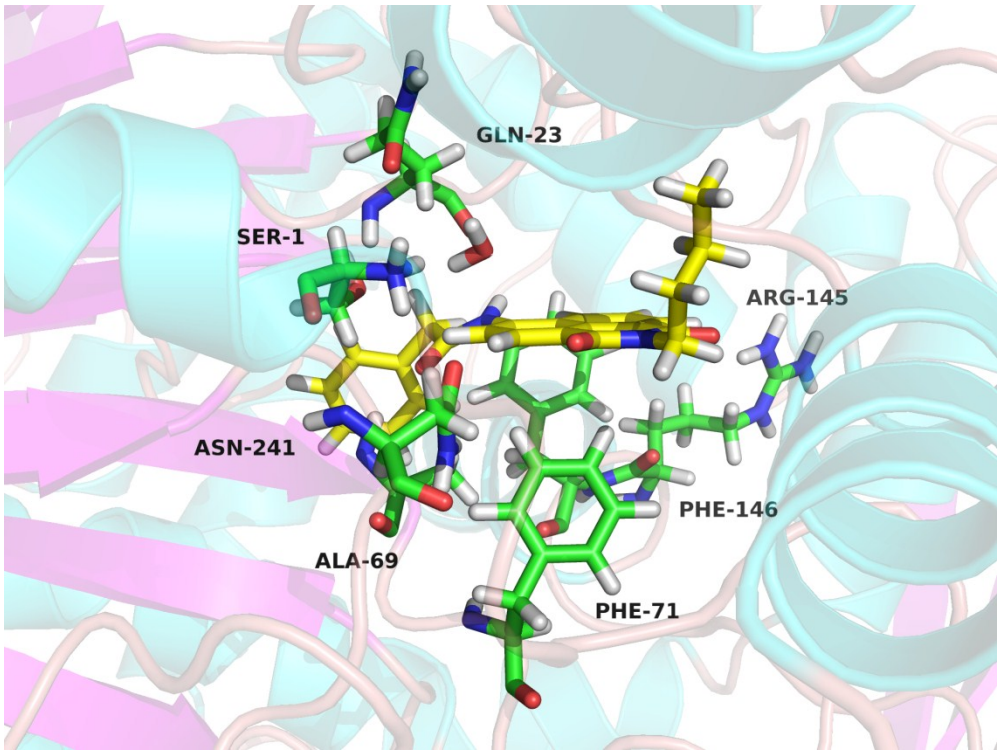

Fig. S3. The docking analysis for fluorescent probe **PNA** and PGA (PDB number: 1FXV).

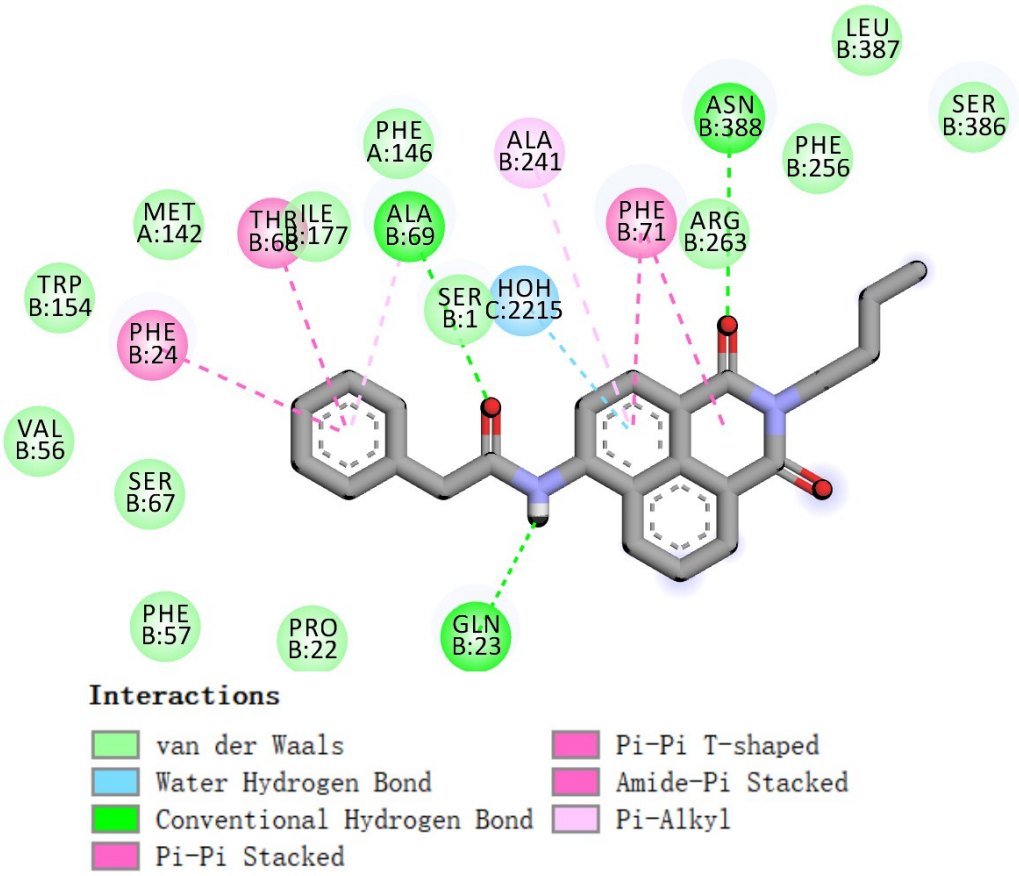

Fig. S4. The interaction between fluorescent probe **PNA** and the amino acid residues of PGA (PDB number: 1FXV).

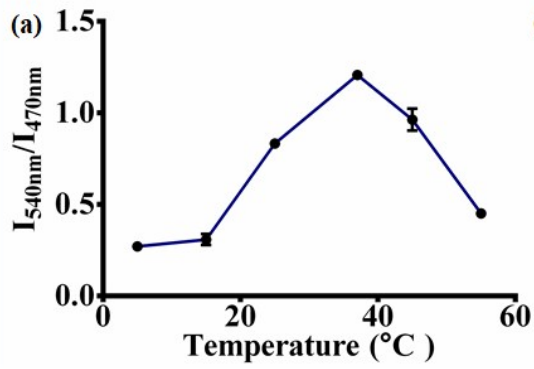

Fig. S5. The hydrolysis of **PNA** (10 μM) mediated by PGA at different incubation temperatures (5, 15, 25, 37, 45, 55 °C; KH_2PO_4-K_2HPO_4 buffer pH 7.4 for 30 min).

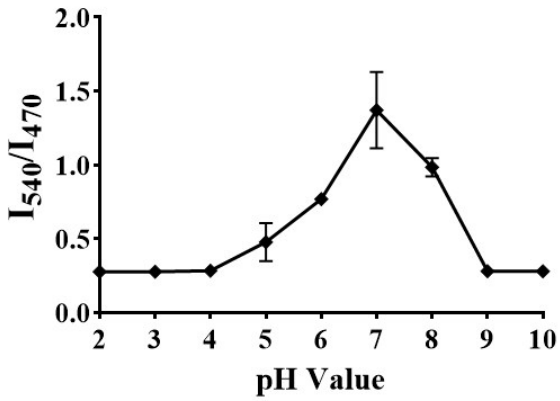

Fig. S6. The fluorescence response of **PNA** toward PGA in KH_2PO_4-K_2HPO_4 buffer with different pH values (2 - 10).

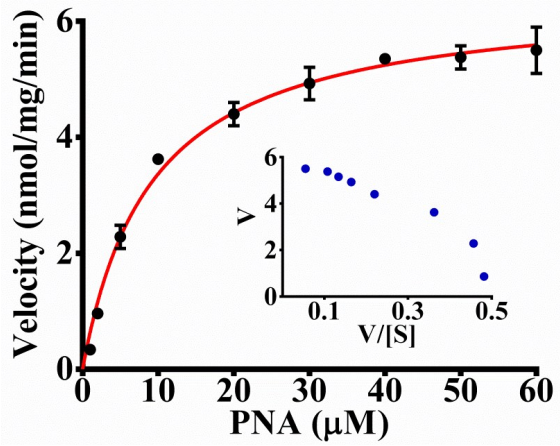

Fig. S7. Kinetic behavior for the hydrolysis of **PNA** mediated by PGA.

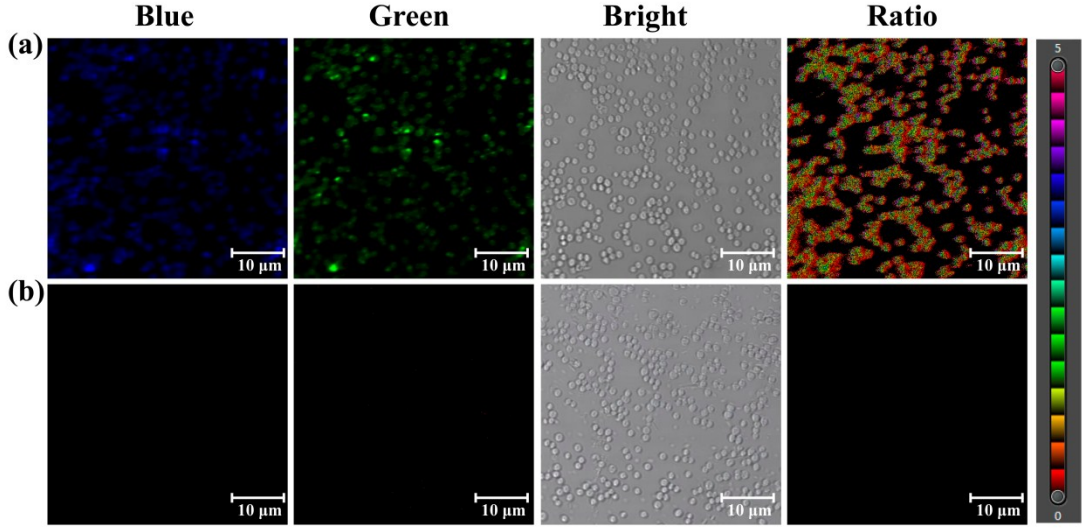

Fig. S8. Fluorescence images of *Staphylococcus aureus* ssp aureus DSM 799 DSM incubated with **PNA** (50 μM). (a) **PNA** (50 μM). (b) Blank group. Blue channel: λ_{ex} 405/λ_{em} 425 – 459 nm, green channel: λ_{ex} 405/λ_{em} 525 – 575 nm. Scale bar 10 μm.

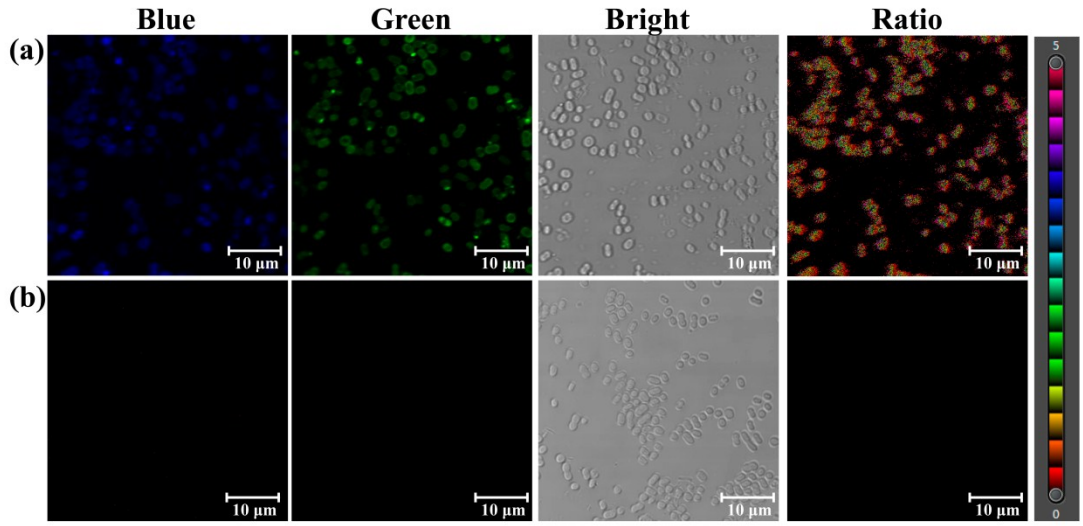

Fig. S9. Fluorescence images of *Acinetobacter baumannii* LMG 994 HAM incubated with **PNA** (50 μM). (a) **PNA** (50 μM). (b) Blank group. Blue channel: λ_{ex} 405/λ_{em} 425 – 459 nm, green channel: λ_{ex} 405/λ_{em} 525 – 575 nm. Scale bar 10 μm.

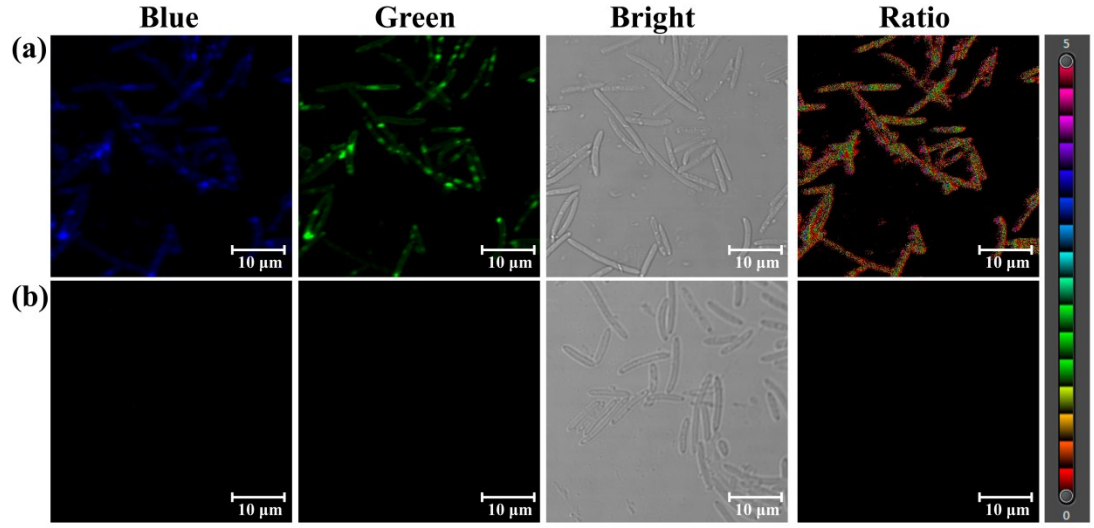

Fig. S10. Fluorescence images of *Brevibacillus parabrevis* 090915_03 LBK incubated with **PNA** (50 μM). (a) **PNA** (50 μM). (b) Blank group. Blue channel: λ_{ex} 405/λ_{em} 425 – 459 nm, green channel: λ_{ex} 405/λ_{em} 525 – 575 nm. Scale bar 10 μm.

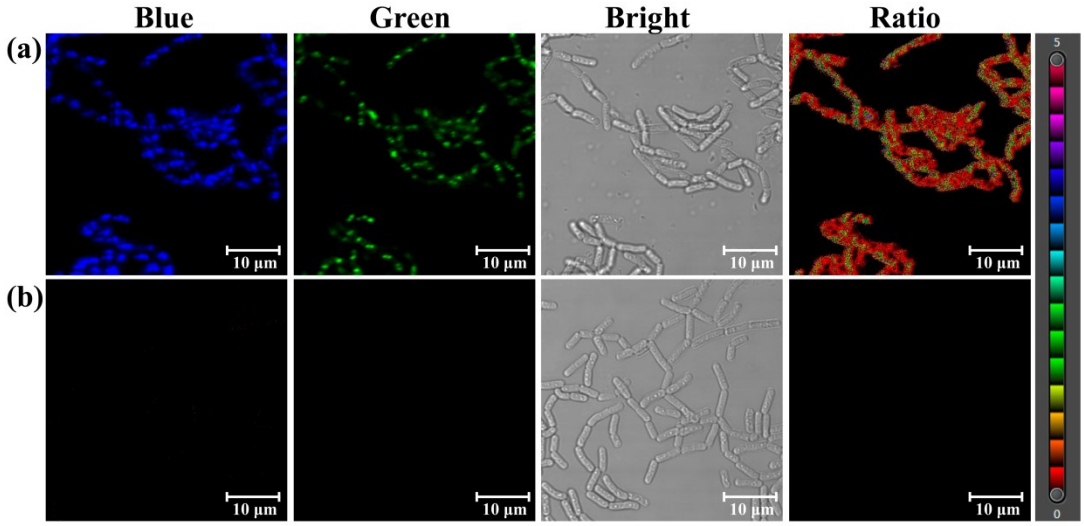

Fig. S11. Fluorescence images of *Bacillus cereus* 994000168 LBK incubated with **PNA** (50 μM). (a) **PNA** (50 μM). (b) Blank group. Blue channel: λ_{ex} 405/λ_{em} 425 – 459 nm, green channel: λ_{ex} 405/λ_{em} 525 – 575 nm. Scale bar 10 μm.

Control	20086-06-0	115-53-7	66-97-7	633-65-8	94-62-2	56-25-7	Control
27208-80-6	81496-81-3	1257-08-5	2415-24-9	58-22-0	13657-68-6	508-02-1	20874-52-6
446-72-0	10338-51-9	305-01-1	546-43-0	531-75-9	128-13-2	472-61-7	257-814-6
501-36-0	568-72-9	529-44-2	530-59-6	84-26-4	1135-24-6	5508-58-7	574-84-5
Control	6093-68-1	7400-08-0	327-97-9	1180-71-8	481-42-5	404-86-4	Control

Figure S12. The CAS number of the natural compounds corresponding to each microplate for inhibitor screening.

Table S1. Information on the natural compounds in the library used for the PGA inhibitor screening.

Compounds	CAS NO.	Compounds	CAS NO.
Coumarins		**Alkaloids**	
Psoralen	66-97-7	Berberine	633-65-8
6,7-Dihydroxycoumarin	305-01-1	Sinomenine	115-53-7
Esculin hydrate	531-75-9	Piperine	94-62-2
Fraxetin	574-84-5	Rutecarpine	84-26-4
6-Hydroxycoumarin	6093-68-1	Capsaicin	404-86-4
Sesquiterpenes		**Phenolics**	
Dihydroartemisinin	81496-81-3	Polydatin	27208-80-6
Curdione	13657-68-6	Salidroside	10338-51-9
Alantolactone	546-43-0	Resveratrol	501-36-0
Monoterpenes		Sinapic Acid	530-59-6
Catalpol	2415-24-9	Ferulic acid	1135-24-6

Diterpenes		p-Hydroxy-cinnamic acid	7400-08-0
Andrographolide	5508-58-7	Chlorogenic acid	327-97-9
Triterpenes		**Quinones**	
Oleanolic acid	508-02-1	Tanshinone IIA	568-72-9
Saikosaponin D	20874-52-6	5-Hydroxy-2-Methyl-1,4-Naphthoquinon	481-42-5
Ginsenoside Re	257-814-6	**Others**	
Flavones		cantharidin	56-25-7
(-)-Epicatechin gallate	1257-08-5	Diosbulbin B	20086-06-0
Genistein	446-72-0	Astaxanthin	472-61-7
Myricetin	529-44-2	Limonin	1180-71-8
Steroids			
Ursodeoxycholic Acid	128-13-2		
Testosterone	58-22-0		

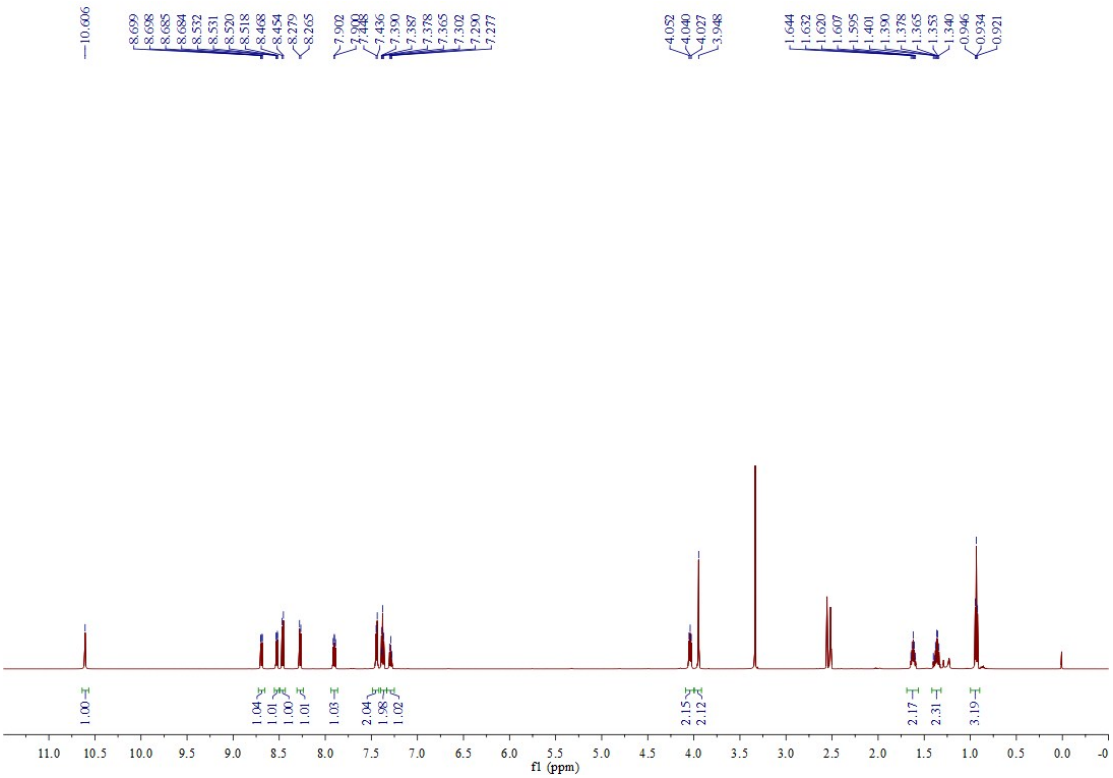

Fig. S13. ^{1}H NMR spectrum (DMSO-d_6, 600 MHz) of **PNA**.

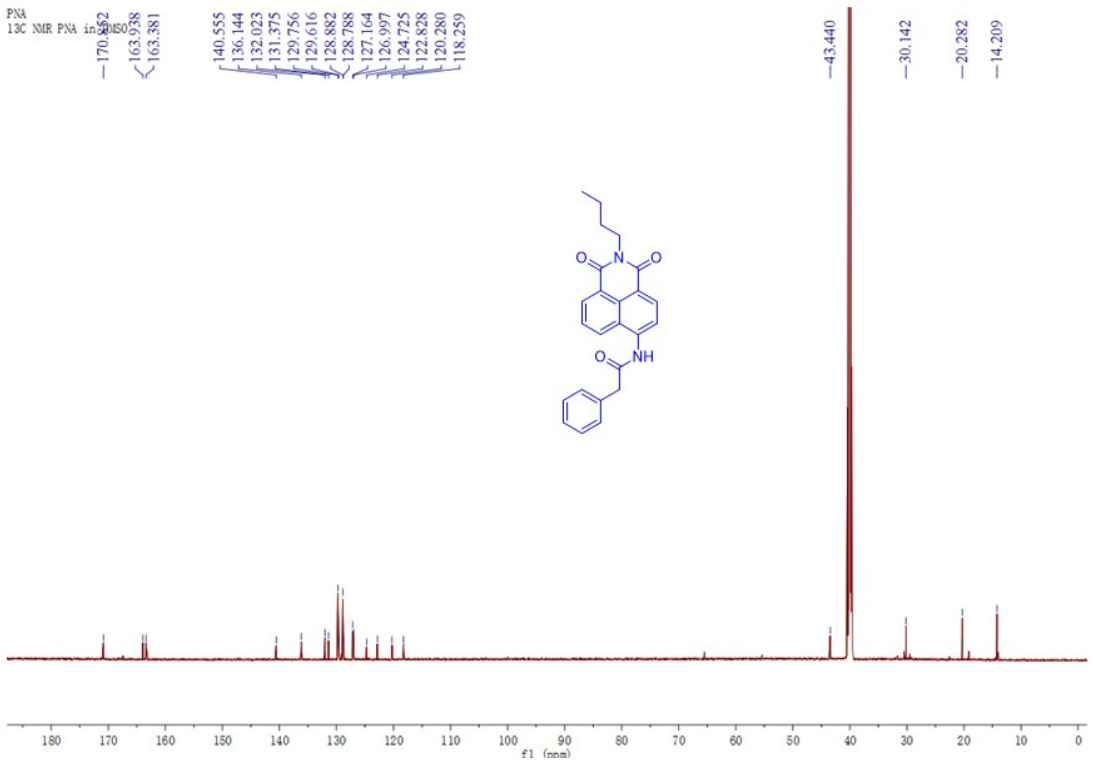

Fig. S14. ^{13}C NMR spectrum (DMSO-d_6, 150 MHz) of **PNA**.

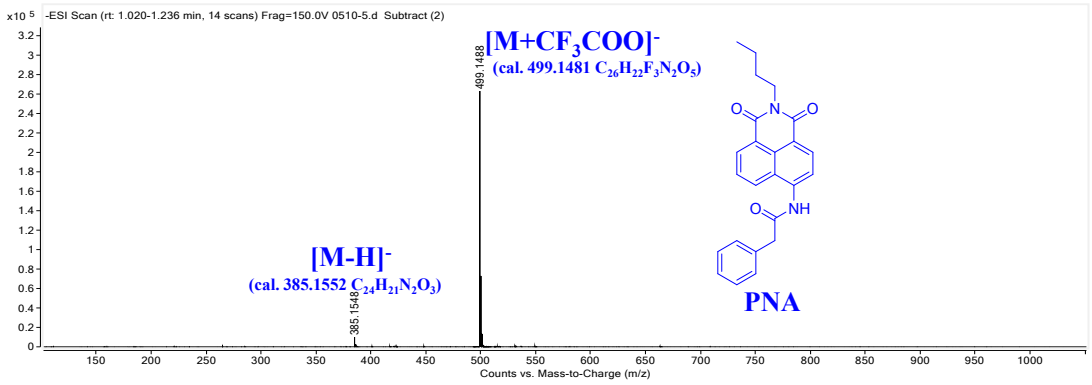

Fig. S15. HRMS of **PNA**.

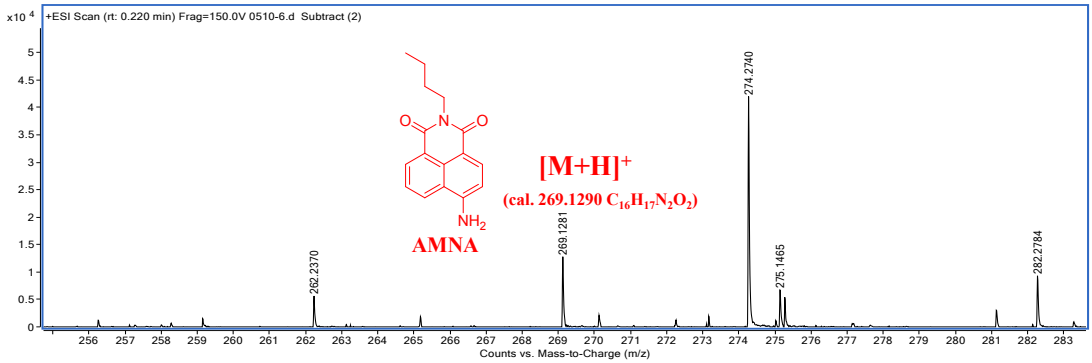

Fig. S16. HRMS of **AMNA**.